24. Interface Marking in Crystals

Experiment MA-060

H. C. Gatos,[a†] A. F. Witt,[a] M. Lichtensteiger,[a] and C. J. Herman[a]

ABSTRACT

Experiment MA-060 was designed to establish the crystal growth and segregation characteristics from the melt in a directional solidification configuration under near-zero-g conditions. The germanium (doped with gallium) system was selected because it has been studied extensively on Earth and because it lends itself to a very detailed macroscopic and microscopic characterization. The interface demarcation technique was incorporated into the experiment because it constitutes a unique tool for recording the morphology of the growth interface into the grown crystal, for determining the microscopic growth rate throughout solidification, and for establishing an absolute time-reference framework for all stages of the solidification process. An extensive study of the germanium crystals grown during the Apollo-Soyuz Test Project was conducted. It was found that single crystal growth was achieved and that the interface demarcation functioned successfully. On the basis of the results obtained to date, there is no indication that convection driven by thermal or surface tension gradients was present in the melt. The gallium segregation, in the absence of gravity, was found to be fundamentally different in its initial and in its subsequent stages from that in the ground-based tests. None of the existing theoretical models for growth and segregation can account for the observed segregation behavior in the absence of gravitational effects. The results strongly suggest the acute need for extensive experimental and theoretical work on Earth before the far-reaching implications of materials processing in space can be understood and exploited.

INTRODUCTION

Gravity-induced convection is always present in the melt undergoing solidification because of unavoidable thermal gradients. It has also been established that thermal convection causes uncontrollable variations in the rate of crystal growth (or solidification), which in turn result in compositional inhomogeneities and structural defects. Thus, gravity adversely affects the key parameters of the crystal growth (solidification) process. Furthermore, thermal convection interferes with the study of the processing parameters (i.e., solidification rate, growth interface characteristics, and others) and with the assessment of the relative importance of such parameters in the physical and chemical characteristics of the resulting solids. Since some key materials processing parameters remain essentially unaffected in the absence of gravitational effects, space provides a unique environment and a striking opportunity for materials processing.

The experiment of indium antimonide (InSb) crystal growth during the Skylab missions demonstrated beyond doubt that, in a zero-g environment, virtually ideal conditions for crystal growth can be established, which lead to chemical homogeneity never attained on Earth, and demonstrated that crystal growth and segregation phenomena can be studied directly in the absence of convective interference. On the basis of the

[a]Massachusetts Institute of Technology.

[†]Principal Investigator.

Skylab findings, the present experiment was designed to obtain more refined fundamental and quantitative information on the crystal growth and segregation processes. The germanium (Ge) (doped with gallium (Ga)) system was selected because it has been the most extensively studied system during the last 30 years. The following subsections discuss experiment results; related technical information is included in the appendix to this section.

OBJECTIVES

The specific objectives of the MA-060 experiment for the Apollo-Soyuz Test Project (ASTP) were to determine the following characteristics under near-zero-g conditions.

1. The absence or presence of convective phenomena
2. The surface tension (and/or wetting) characteristics of the melt
3. The microscopic growth-rate behavior during directional solidification
4. The dopant segregation behavior and its dependence on the microscopic growth rate
5. The heat-transfer characteristics of the solidification system

EXPERIMENTAL APPROACH

To achieve the experimental objectives, single crystals grown on Earth were partially melted and resolidified in space with simultaneous transmission of periodic current pulses across the crystal-melt interface.

The in-flight growth experiments were conducted in the multipurpose furnace (fig. 24-1) originally designed for the Skylab missions (ref. 24-1) and modified for ASTP to meet the higher temperature requirements. The stainless-steel cartridges containing the crystal assemblies were inserted into the three tubular cavities of the furnace. Heat levelers, lateral heat shields, and a heat-extraction system controlled the heat flow from the heating element through the crystal to the heat-extractor plate. With the furnace in this configuration, melting was initiated when appropriate power was applied at the crystal end located within the heating element, and the crystal-melt interface was stabilized after 6 cm of each of the original crystals was melted. Stabilization of the crystal-melt interface (thermal soaking) was achieved by reducing the power duty cycle to 90 percent. After thermal soaking (2 hours), the power system was switched to the cooldown mode, resulting in an average cooling rate of 2.4 K/min (2.4° C/min). This cooling rate was expected to yield a microscopic growth rate ranging from 5 μm/sec at the beginning to 10 μm/sec at the end of the controlled cooldown period. Controlled cooldown was terminated after 1 hour and 23 minutes (estimated regrowth length of approximately 4 cm); the growth system was subsequently switched to the passive cooldown mode for 1 hour and 7 minutes, after which helium was injected into the furnace to accelerate the cooling rate.

To permit growth-interface demarcation (ref. 24-2) by current pulsing, leads were attached to the encapsulated Ge crystals. This was achieved with "graphite cup" electrodes at both ends of the crystals to which platinum leads were attached (fig. 24-2). The platinum leads of the three growth systems were connected in series, with the seed having a positive polarity. A power supply provided 19.1-A/cm^2 current pulses of 55-millisecond duration at 4-second intervals throughout the experiment. The specific cartridge design and the optimized interface-demarcation procedure were established during extensive ground-based tests.

RESULTS AND DISCUSSION

Upon return to Earth, the crystals grown in space were subjected to an exhaustive growth and segregation analysis based on procedures established during ground-based tests. The primary analytical techniques used were high-resolution etching, Hall-effect measurements, spreading-resistance measurements, and ion-microprobe analysis. Because of the confined geometry that leads to stresses during growth, no defect analysis of the regrown material was performed.

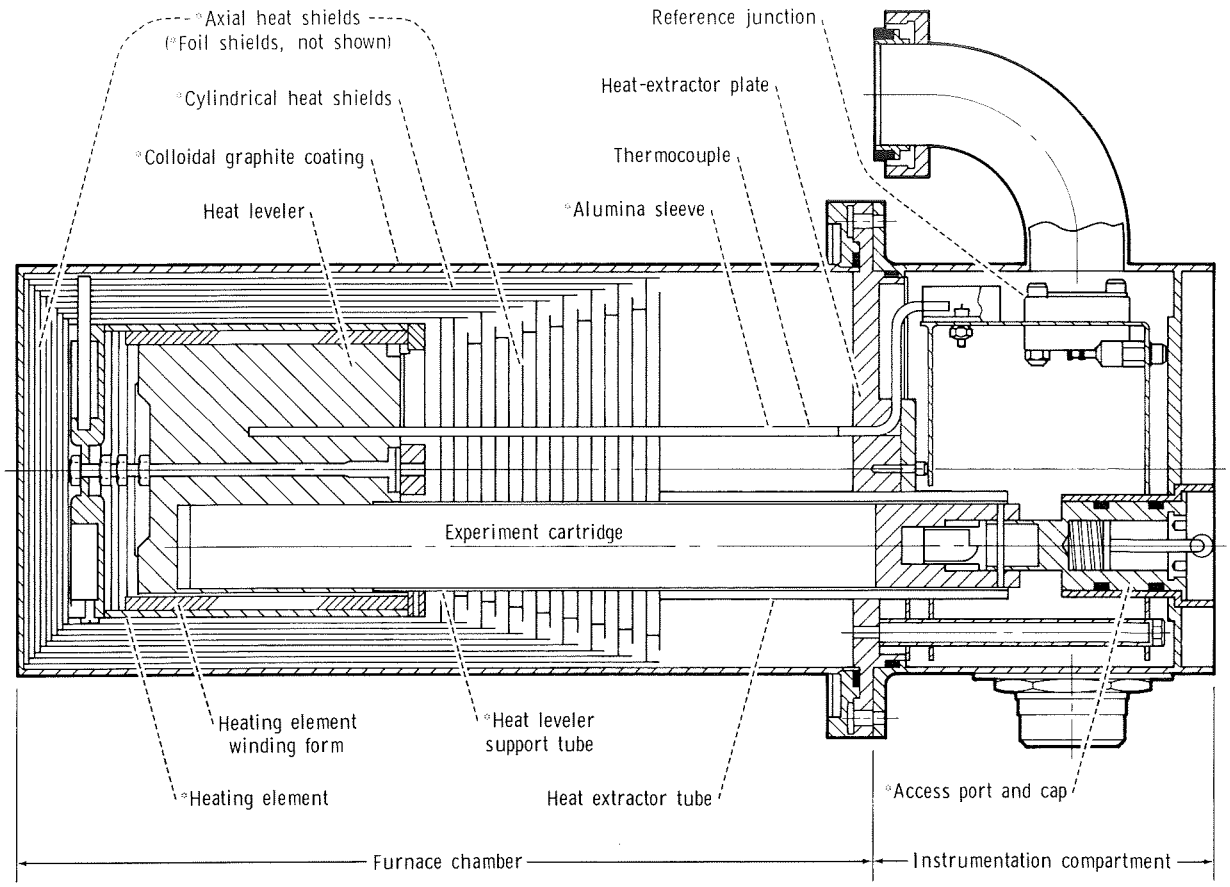

FIGURE 24-1.—Schematic of the multipurpose furnace used for the ASTP crystal growth and solidification experiments. An asterisk indicates design modifications.

Surface Characterization

All crystals regrown in space could readily be removed from their quartz ampoules (fig. 24-3). In contrast, all crystals grown on Earth could be isolated only by dissolving the quartz ampoules in hydrofluoric acid. This pronounced difference in the behavior of the Earth- and space-grown crystals can be understood on the basis of the morphological characteristics of their surfaces. In interference contrast, it was observed that the surfaces of the space-grown crystals exhibited an irregular network of narrow ridges (fig. 24-4) similar to that observed on InSb crystals grown on Skylab. However, all crystals grown during ground-based tests in the same growth facility exhibited surface features that reflected in detail the unavoidable irregularities of the inner walls of their quartz ampoules. It was therefore concluded that no wetting contact existed between the Ge melts and the confining quartz ampoules during growth in space; whereas, during growth on Earth, the Ge melt was in wetting contact with its confinement. This conclusion is significant because it suggests that effective wetting inversion (first observed during growth of InSb during Skylab) is a phenomenon that may be expected to occur in a multitude of systems subjected to solidification in space. The implications of this effect on materials processing are far reaching with regard to processing technology and possibly to the perfection of materials solidified in partial or total confinement.

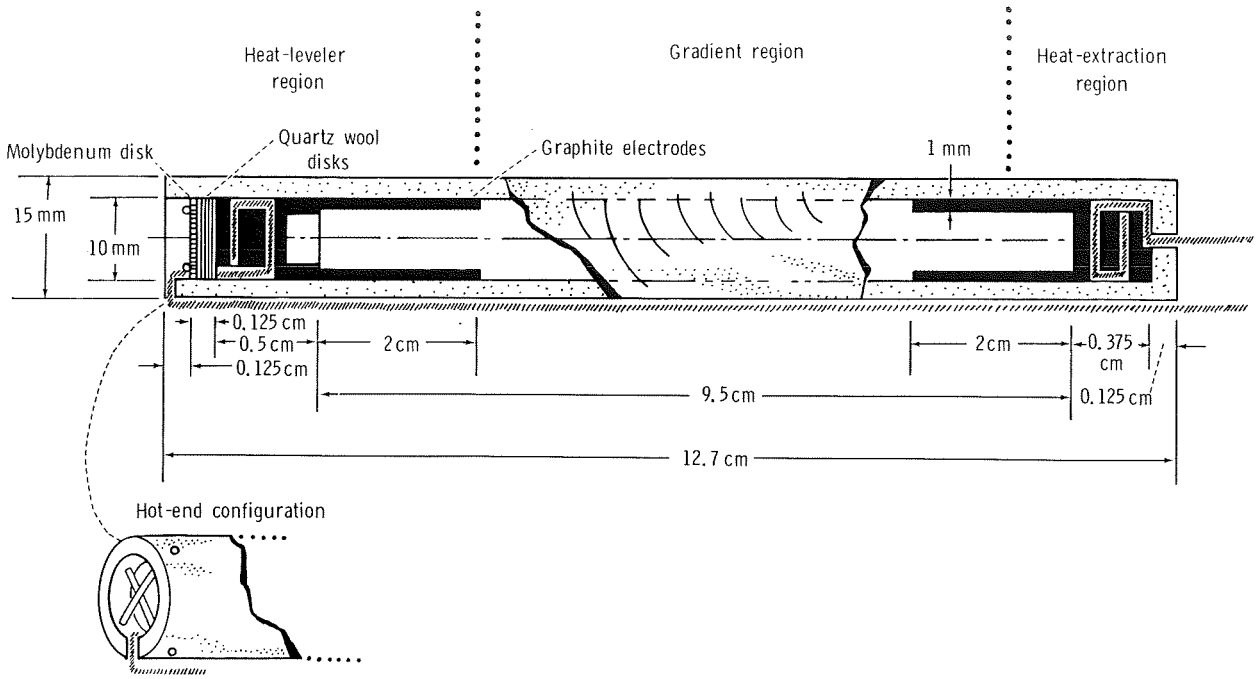

FIGURE 24-2.—Ampoule design permitting interface demarcation through current pulsing during regrowth.

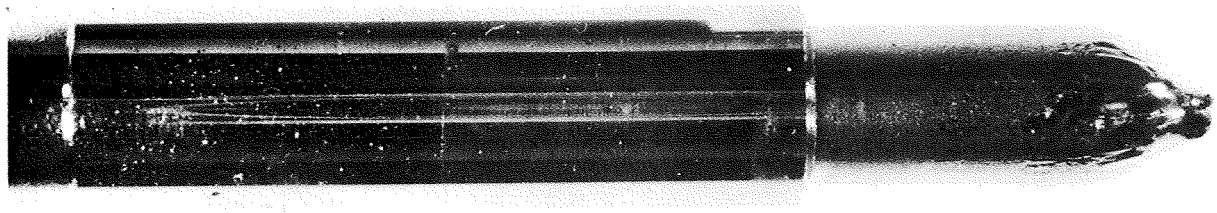

(a)

(b)

FIGURE 24-3.—Germanium crystals regrown in space (after removal from their quartz ampoules). (a) <100> orientation. (b) <111> orientation.

In all crystals, the original regrowth interface was identified (fig. 24-3) and appeared as an abrupt increase (0.5 mm) in crystal diameter at the predicted distance of approximately 3.5 cm from the cold end of the crystals. The location indicates the extent of backmelting in space and confirms on a macroscale the proper functioning of the multipurpose furnace.

From the morphological characteristics (absence of twin and grain boundaries), it is evident that single crystallinity in the peripheral region of the space-grown Ge crystal of <111> orientation prevailed over the entire length of regrowth. In this respect, growth in space and growth on Earth are conspicuously different because crystals regrown during ground-based tests did not exhibit single crystallinity beyond regrowth of approximately 3 cm. The preservation of single crystallinity in the peripheral region (single crystal shell) is particularly remarkable in view of the high doping level at which interface instability (due to constitutional supercooling and eventual interface breakdown) is predicted, in fact observed, in the crystal interior. Single crystallinity in the peripheral region was not preserved on the space-grown <100> crystal. In this case, grain boundaries were first observed after growth of 3.5 cm, which compares favorably with ground-based tests in which breakdown first occurred after approximately 2 cm of growth.

Bulk Characterization by High-Resolution Etching

High-resolution etching techniques were refined during ground-based tests to permit the detection of microscopic compositional fluctuations in Ge with a sensitivity of more than ±0.2 percent at Ga-dopant levels in excess of 10^{18}/cm.

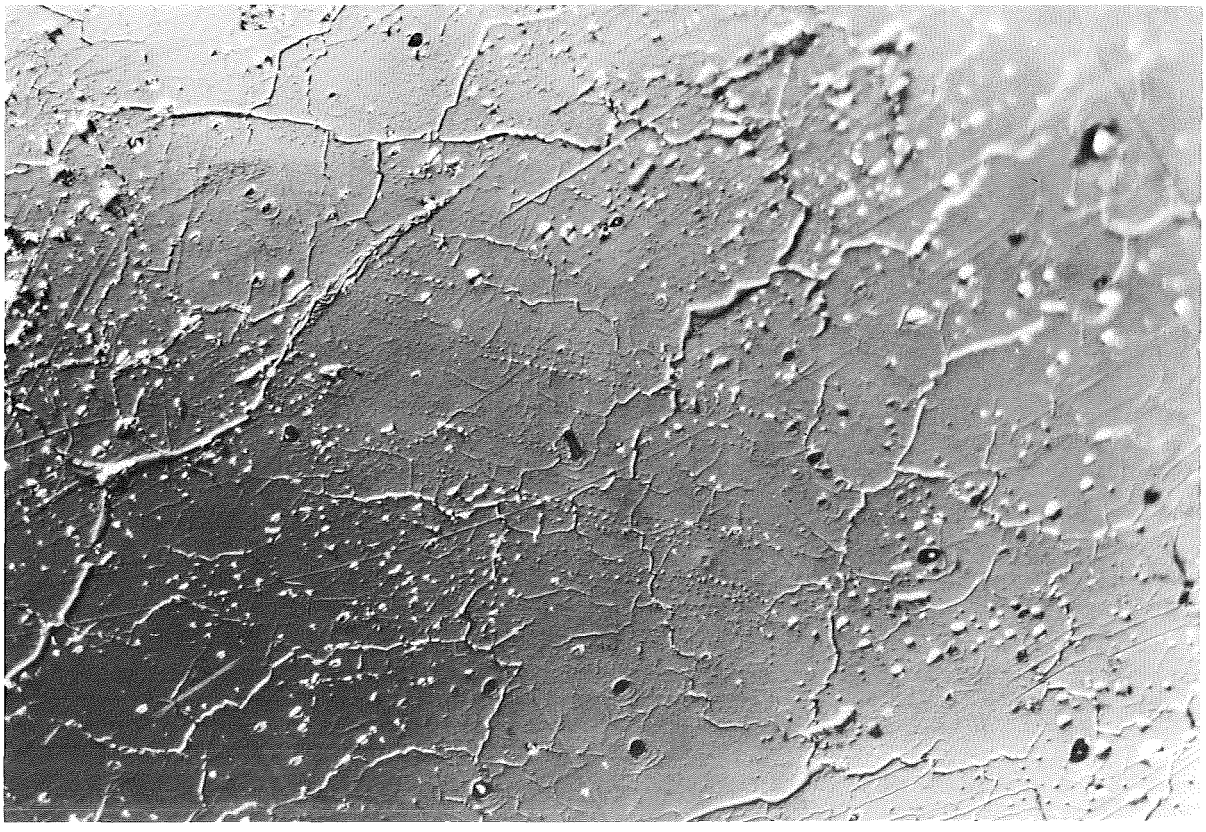

FIGURE 24-4.—Irregular ridge patterns on the surface of the <100> Ge crystal regrown in space. (Magnification of 123× .)

Bulk characterization by etching was performed on longitudinal center cuts of the regrown segments. The exposed surfaces were polished and etched. An etched segment of the <111> Ge crystal regrown in space is shown in figure 24-5. Three regions can be identified: the original seed portion (top), a narrow region exhibiting microscopic compositional inhomogeneities (center), and a region exhibiting no compositional fluctuations (bottom). The latter growth region exhibits faint, but distinct, lines that are the current-induced interface demarcations formed at 4-second intervals during regrowth. The spacing of consecutive demarcation lines can be seen to converge to zero (zero growth rate) at the lower end of the bandlike region of perturbed growth and segregation. Thus, interface demarcation established that the formation of the growth region with compositional fluctuations (band below the original regrowth interface) occurred during the 2-hour thermal soak and preceded the controlled regrowth. Ground-based tests indicated that this growth band reflects thermal instability of the furnace and is attributed to a slight imbalance of heat input and heat loss during the early thermal soak stages.

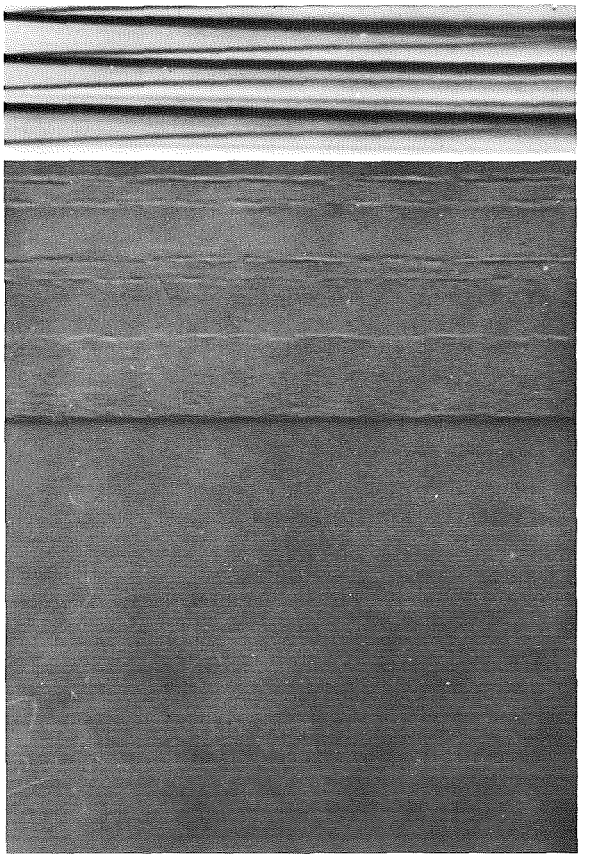

FIGURE 24-5.—Etched segment of the <111> Ge crystal regrown in space. Note the seed portion (top) and the controlled regrowth portion (bottom) separated by a band of uncontrolled growth and segregation. (Magnification of 72×.)

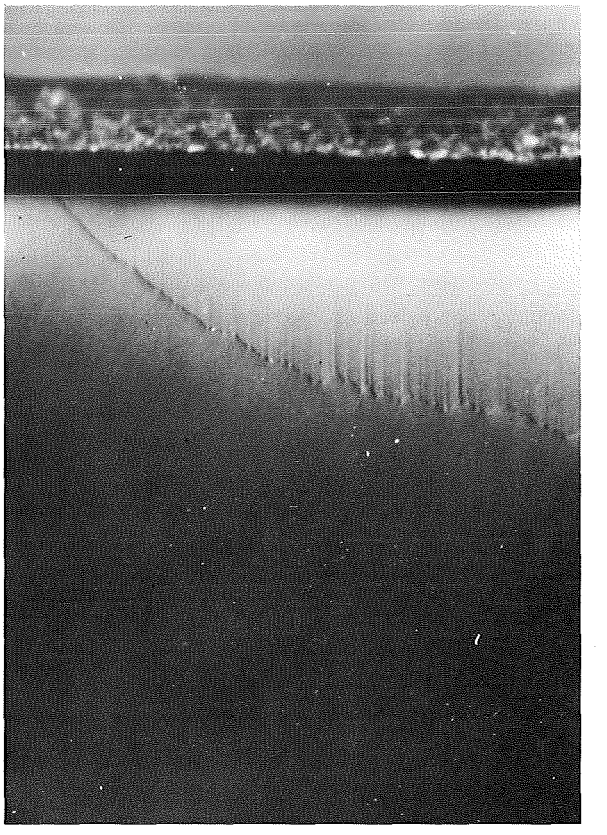

FIGURE 24-6.—Segregation inhomogeneities associated with peripheral facet formation in the <111> Ge crystal regrown in space. (Magnification of 182×.)

Etching analysis revealed further that the bulk of the controlled regrowth region of the <100> crystal was free of microscopic compositional fluctuations over a growth length of more than 2.5 cm. For regrowth in the <111> direction, minor compositional fluctuations of approximately 0.1 percent were observed associated with peripheral

facet formation (fig. 24-6). The nature of these perturbations is not yet understood.

Segregation inhomogeneities associated with interface breakdown due to constitutional supercooling were observed in all crystals after the advancing growth front had moved into the graphite cup. The breakdown in the space-grown material was attributed to deteriorating thermal gradients caused by abrupt changes in the thermal conductivity of the confinement system (in going from quartz to graphite) and the resulting changes in the growth-interface morphology. It is important to note that the onset of instability occurred significantly earlier in the <111> crystal and was initiated at the facet to off-facet boundary. Occasionally, the morphological characteristics of the unstable growth interface were much more regular and conforming to theoretical predictions in the space-grown crystals than they were in the Earth-grown crystals (fig. 24-7).

Growth-Rate Behavior on the Microscale

From interface demarcation lines introduced at 4-second intervals, a quantitative growth-rate analysis on a microscale was performed for all space-grown crystals. The growth-rate data for the crystal grown in the <111> direction are shown in figure 24-8. Notice that, during the early stages of the cooling cycle, the microscopic growth rate increased rapidly from 0 μm/sec to approximately 7 μm/sec. After the initial transient region, the rate increase slowed down and, after approximately 2.5 cm of growth, the microscopic growth rate approached 10.5 μm/sec. The growth-rate behavior observed in space (for the cooling rate of 2.4 K/min (2.4° C/min)) was virtually identical with that encountered during ground-based tests and indicates that the heat-transfer characteristics of the system are the same in space as they are on Earth. This result indicates that, in the growth configuration used, conductive heat transfer dominates and that the contribution of laminar convection to heat transport, which is present in the ground-based tests, is negligible.

It should be pointed out that all existing theories of segregation assume an initial step function of the growth rate from zero to a finite and constant rate; however, because all real melt-growth systems exhibit an initial transient growth behavior, no quantitative comparison between theory and experiment can be made. In view of these results, the development of a modified segregation theory has been initiated that considers the existence of initial growth-rate transients under convection-free conditions.

Dopant Segregation Behavior

Quantitative compositional analyses of crystals regrown in space and on Earth have been obtained by means of spreading-resistance measurements with a linear resolution of 5 μm. The results obtained for the initial regrowth region of crystals grown in the <111> direction are shown in figure 24-9. (These regions are the same as those shown in fig. 24-5.) The measurements obtained along the growth direction of an Earth- and space-grown sample identify three regions: the seed regions (marked left), characterized by pronounced compositional fluctuations; the bands of uncontrolled growth (marked center); and the regrown regions with steadily increasing dopant concentration (marked right). Notice that the initial region in the space-grown crystal exhibits a much more rapid dopant concentration increase than the Earth-grown crystal. This behavior reflects the effect of laminar convection on segregation. The results are not, however, as expected with regard to the absolute dopant concentration level. Assuming the equilibrium distribution coefficient k_o of Ga in Ge to be 0.087 (as generally accepted), the dopant concentration in the initial regrowth region should assume a value of approximately $9 \times 10^{17}/cm^3$ instead of the presently measured value of $2.43 \times 10^{18}/cm^3$. Since virtually identical initial dopant concentration levels were observed in both samples, the generally accepted value for k_o was assumed to be erroneous.

The appearance of growth facets in the space-grown <111> crystal enabled the study of facet-segregation behavior in the absence of convective interference. The spreading-resistance measurements (fig. 24-10) show that the dopant concentration on-facet is less than that off-facet by a factor of 0.92. The tracings also show that the

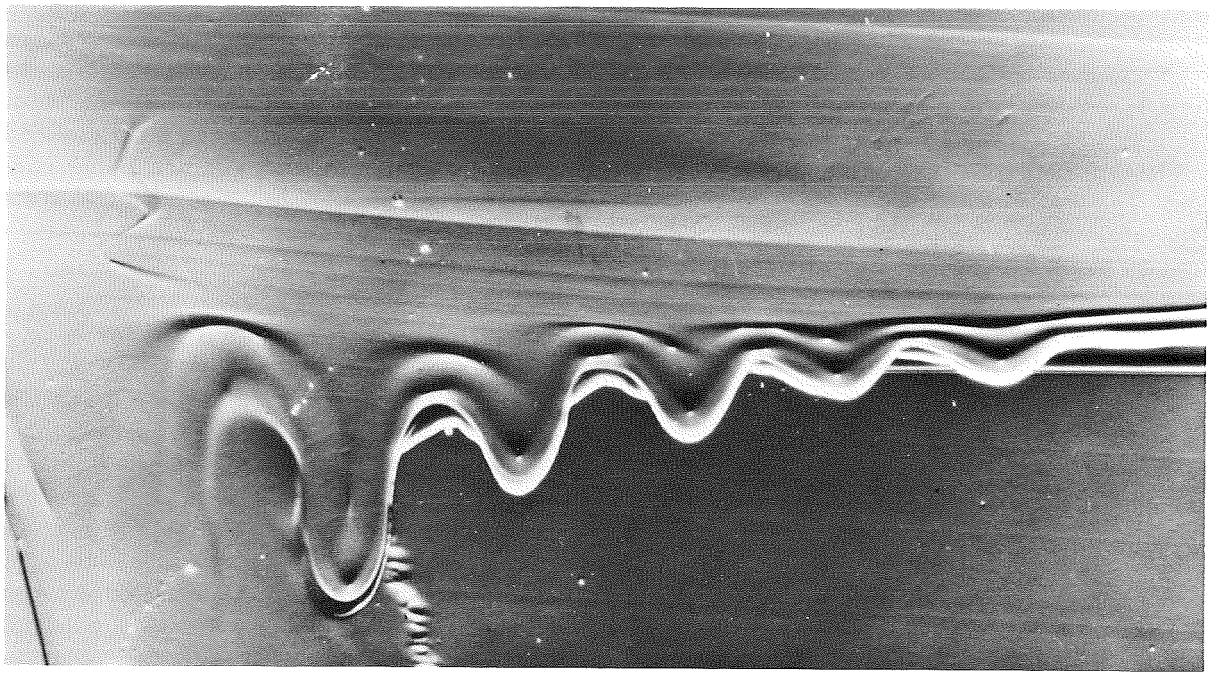

(a)

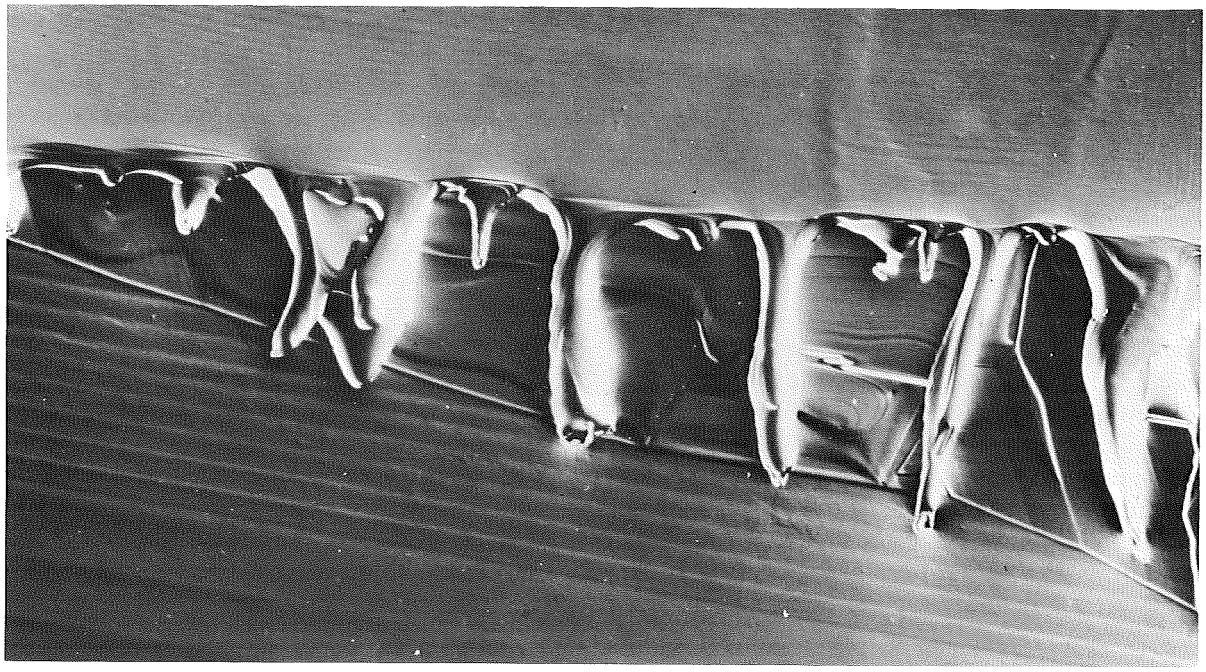

(b)

FIGURE 24-7.—Frontal interface breakdown during late stages of <111> Ge regrowth. (Magnification of 200×.) (a) Space-grown. (b) Earth-grown.

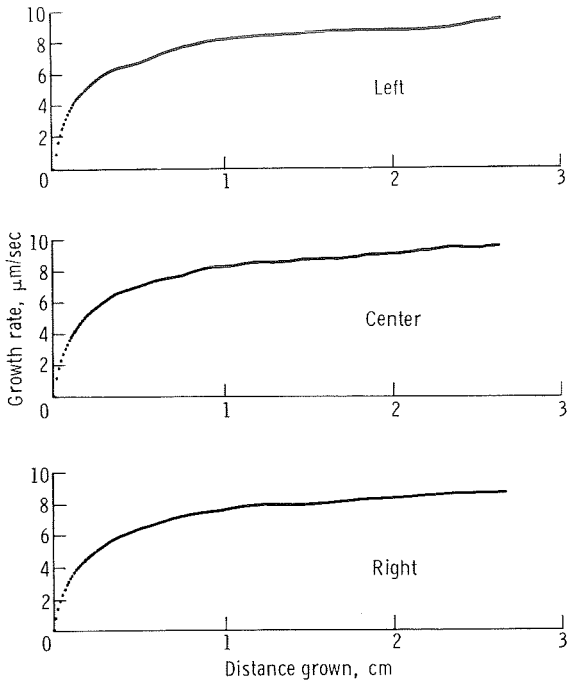

FIGURE 24-8.—Microscopic growth rates of the <111> Ge crystal regrown in space.

compositional change on-facet to off-facet occurs over a distance of approximately 30 μm.

Attempts to analyze quantitatively the initial segregation transient in the regrowth region of the space-grown sample were unsuccessful because of the existing growth-rate transient that is not considered in the theoretical treatments. Because of the unavailability of reliable values for k_o and for the diffusion coefficient D (essential for a quantitative segregation analysis), appropriate experiments must be conducted under zero-g conditions to accurately determine these constants.

Compositional analysis on a macroscale, covering the entire length of crystals regrown in space, is still being conducted. The results obtained to date are largely unexpected and as yet unexplained. As shown in figure 24-11, the dopant concentration, as expected, increased steadily over a distance of approximately 1.5 cm from the original regrowth interface. At this distance, the effective distribution coefficient k_{eff} approached the value of 1, which is characteristic of diffusion-controlled steady-state segregation. However, with continuing growth and with a steadily increasing microscopic growth rate, the dopant concentration decreased instead of reaching the steady-state value. The dopant concentration continued to decrease over a distance of approximately 1 cm of growth. At this point, interface breakdown due to constitutional supercooling occurred and a further analysis of the segregation behavior was not possible.

There are indications that the observed segregation anomaly is not characteristic of growth under zero-g conditions, but that it was a consequence of the particular geometry of the growth system. In view of the potentially far-reaching implications of these unexpected segregation effects, a complete understanding of their origin is of paramount importance.

SUMMARY

The results of the MA-060 experiment revealed growth and segregation effects previously not observed on Earth. The majority of these effects cannot be explained by any existing experimental or theoretical models of growth and segregation. This finding has fundamental implications because germanium is the most studied and best understood of all solids. The clear implication is that, although space provides a unique environment for materials processing, exploitation of the unprecedented opportunities of the zero-g environment necessitates the selection of systems and experimental apparatus that have been, or can be, exhaustively investigated on Earth so that zero-g effects on materials processing can be unambiguously identified and quantitatively studied. In addition, extensive research is essential following space experimentation (even on critically selected and well-understood systems) to quantitatively understand the zero-g effects and establish sound guidelines for subsequent space processing. The authors believe that materials processing in the Space Shuttle Program could be a most expensive and unprofitable undertaking unless ground-based investigations on critically selected materials systems are greatly expanded.

The following material represents an update to the preceding analysis and was added after proofreading.

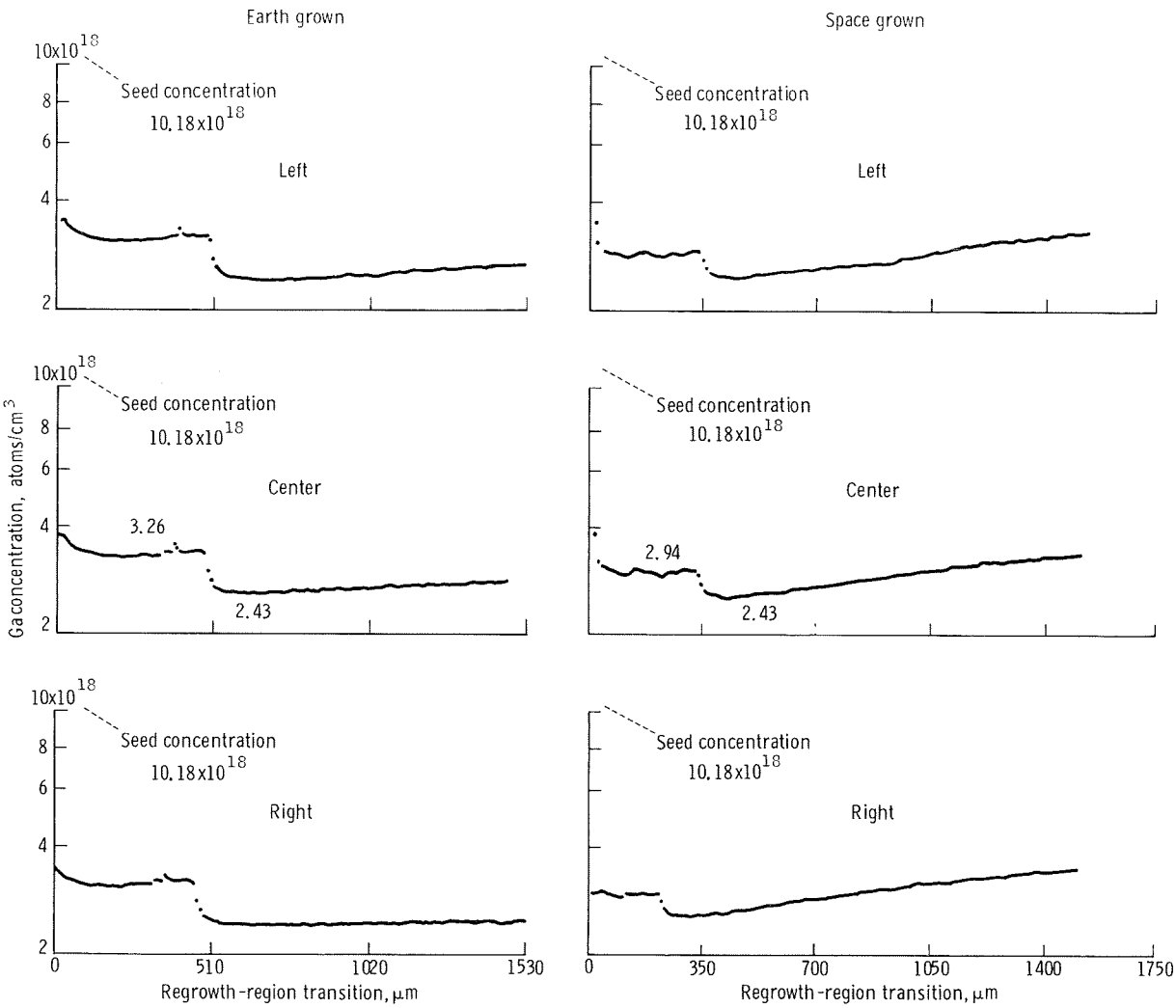

FIGURE 24-9.—Compositional profiles of the initial regrowth region in the <111> Ge crystal regrown in space. (Ground-based data are shown for comparison.)

MACROSEGREGATION ANALYSIS

A comprehensive macrosegregation analysis for both Ga- and Sb-doped Ge crystals grown in space was conducted. It was found that the previously unexplained segregation effects are directly related to the characteristics of the growth interface morphology which in turn are controlled by the thermal configuration provided in the multipurpose furnace. In addition, the analysis showed that the dopant distribution in Ga-doped crystals grown in space is in all respects consistent with diffusion-controlled segregation. The observed segregration behavior provides no evidence of convection in the melt.

The compositional profiles for the first 2.5 cm of Ga- and Sb-doped Ge crystals grown in space are shown in figure 24-12. These data were obtained from spreading resistance measurements on longitudinal cuts containing the growth axes of the crystal. It can be seen that dopant segregation in both systems has the same basic characteristics: the dopant concentration increases steadily in the direction of regrowth, indicative of transient

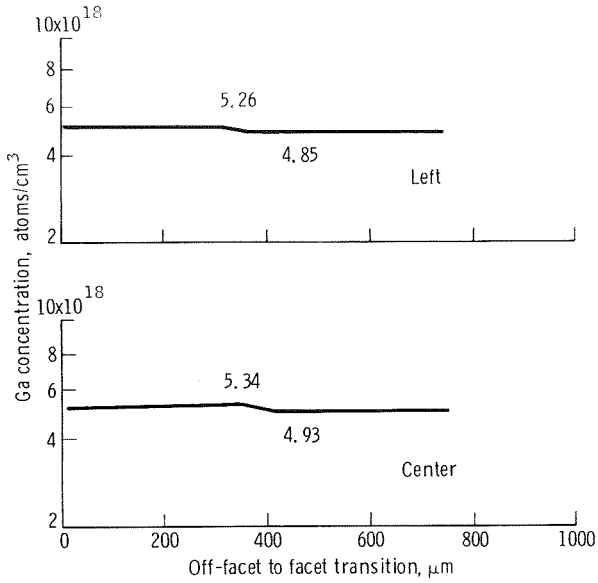

FIGURE 24-10.—Compositional profile of the off-facet to facet transition region in the <111> Ge crystal regrown in space.

segregation and consistent with theory. The concentration profiles of both systems show, in addition, longitudinal and radial compositional variations for which the origin could not be explained previously. Of particular concern was the Ga-concentration decrease on the right and center scans of figure 24-12(a), first noticeable at a distance of approximately 1.3 cm from the original regrowth interface. Since this concentration decrease reflects a net decrease of the dopant concentration within the diffusion boundary layer (the microscopic growth rate is still steadily increasing), it could be interpreted as indicative of convective interference. To assess, for the analyzed growth region, the magnitude of effective segregation, average longitudinal dopant concentration profiles were determined by averaging along the growth direction the corresponding concentration values of the left, center, and right scans of figures 24-12(a) and 24-12(b). It is seen in figure 24-13(a) that the averaged dopant concentration profile does not exhibit the pronounced compositional variations observed in the longitudinal scans of figure 24-12(a). The minor compositional variations observed in figures 24-13(a) and 24-13(b) are considered as deficiencies of the averaging process, which by necessity is confined to one plane of the cylindrical crystal. Thus, it is concluded that the concentration variations observed on the longitudinal scans at distances in excess of 1 cm from the original regrowth interface do not constitute changes in segregation brought about by dopant depletion within the diffusion boundary layers; but, rather, that they reflect radial dopant redistribution within the diffusion boundary layer.

As indicated in figure 24-12, the dopant concentration in both systems is radially uniform at the onset of regrowth. With continuing growth, a radial nonuniformity in composition develops with the dopant concentration in the center exceeding significantly that on the periphery. At a distance of approximately 0.3 cm from the original regrowth interface it becomes apparent that radial segregation is asymmetric and, with continuing growth, undergoes pronounced changes. A study of the growth interface morphology (made possible through interface demarcation) reveals that the radial dopant incorporation is in all respects consistent with diffusion-controlled segregation on a nonplanar growth front; thus, the originally established growth interface, which is concave into the crystal, will result in a correspondingly curved boundary layer. Since the diffusive dopant flux away from the growth interface is largest in the normal direction, it will result in a nonuniform dopant distribution within the diffusion boundary layer and correspondingly lead to radially nonuniform dopant incorporation in the growing crystal.

In view of the interdependence of growth interface morphology and radial dopant segregation under diffusion-controlled conditions, a detailed study of the morphology of the crystal melt interface and its changes during growth was conducted. It was found that the growth interface (in both crystals analyzed) is axially asymmetric and changes continuously with growth. In particular, it was observed that pronounced morphological changes take place when the growth interface is located in the region where the radial temperature control changes from axial heat shields to the heat leveler. A comparison of the growth interface morphology and its changes during growth with

radial dopant segregation indicates in all instances a behavior that is consistent with diffusion-controlled dopant redistribution within the diffusion boundary layer.

The preceding analysis, together with the observed compositional homogeneity on a microscale, must be taken as conclusive evidence for the absence of time-dependent convective flows in the Ge melt under the presently used growth configuration.

In the context of the present study, it is important to recognize that time-independent convective melt flows are only consequential if they affect macrosegregation and prevent the establishment of dynamic steady-state conditions for which k_{eff} becomes 1 and the composition of the growing crystal becomes constant. Thus, unambiguous evidence for the absence of convective interference with segregation is given by the achievement of constant composition in a grown crystal—as reported for InSb crystal growth during the Skylab missions. In the presently studied systems, because of the small dopant distribution coefficients, constant composition cannot be achieved over the limited growth length; thus, the analysis for residual convection effects must be based on the segregation behavior in the transient region.

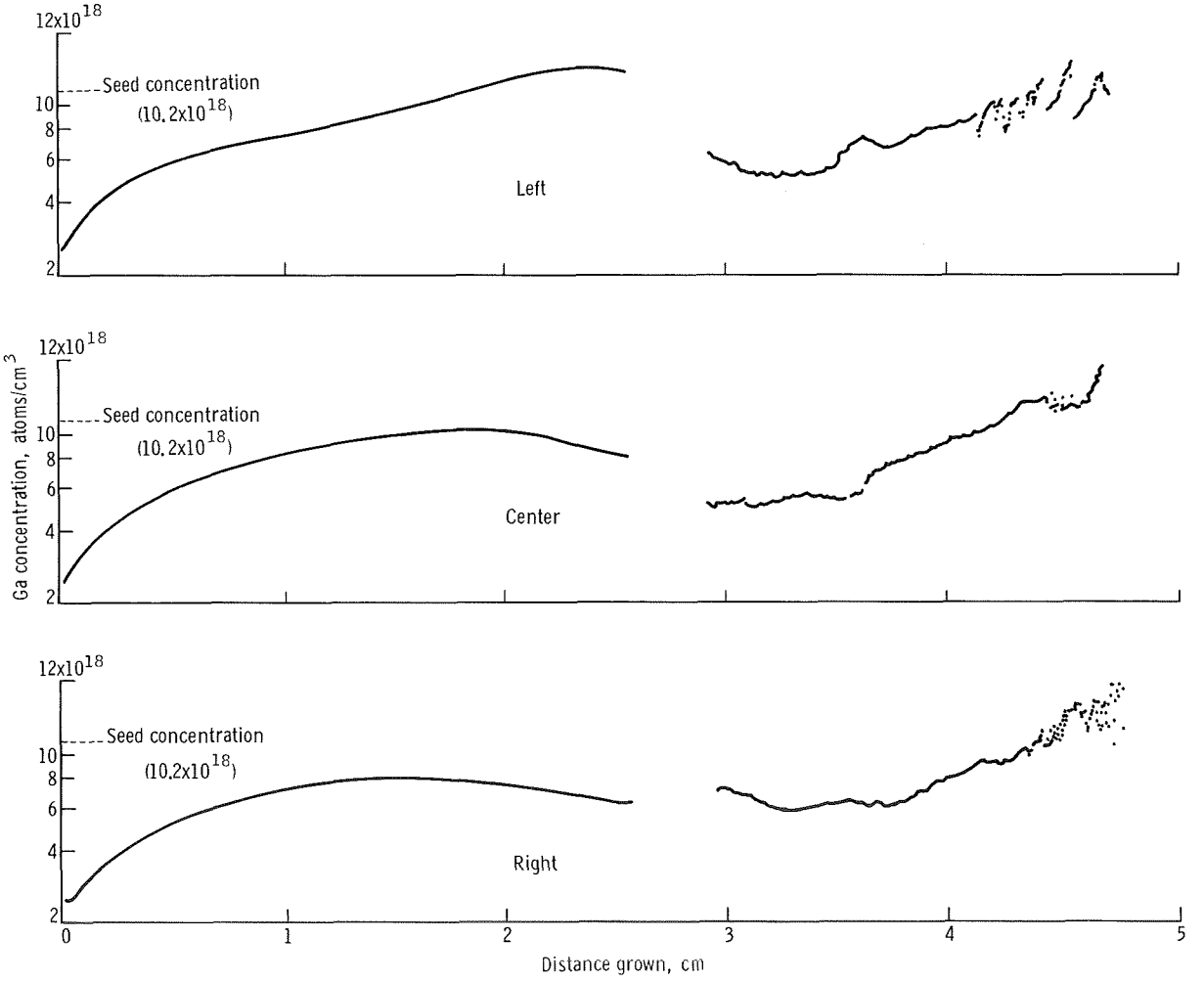

FIGURE 24-11.—Macroscopic compositional profile of the <111> Ge crystal regrown in space.

Such an analysis, as indicated earlier, is complicated by three facts: (1) The transient region is associated with a steadily increasing growth rate—conditions for which the theoretical transient segregation in the absence of convection has, as yet, not been determined; (2) the diffusion coefficients for Ga and Sb in Ge melts are not known with adequate precision; the best published data for diffusion of Ga in Ge range from $D = 7.5 \times 10^{-5}$ to 1.5×10^{-4} cm^2/sec; and (3) the generally accepted equilibrium distribution coefficients for Ga in Ge range from $k_o = 0.087$ to 0.12.

Although the existing theoretical treatment of transient segregation in the absence of convective interference (ref. 24-3) assumes a constant rate of growth, it can nevertheless be usefully applied to the present results. According to this theory, the dopant concentration in the growing solid will assume the value C_x at a distance x from the original regrowth interface

$$C_x = C_L \left\{ \left(1 - k_o\right) \left[1 - \exp\left(-k_o \frac{R}{D} x\right) \right] + k_o \right\} \quad (24\text{-}1)$$

where R is the microscopic rate of growth and C_L is the concentration in liquid. For $x = D/(k_o R)$ (the characteristic distance), C_x becomes

$$C_x = C_L \left[\left(1 - k_o\right) \left(1 - \frac{1}{e}\right) + k_o \right] \quad (24\text{-}2)$$

Therefore, by using a value of R as the average measured value of 7×10^{-4} cm/sec, it is possible to determine a characteristic distance range (x_{min} and x_{max} controlled by the spread of accepted values of D and k_o) over which, in the absence of convective interference, the dopant concentration in the solid melt must have risen to the value of C_x.

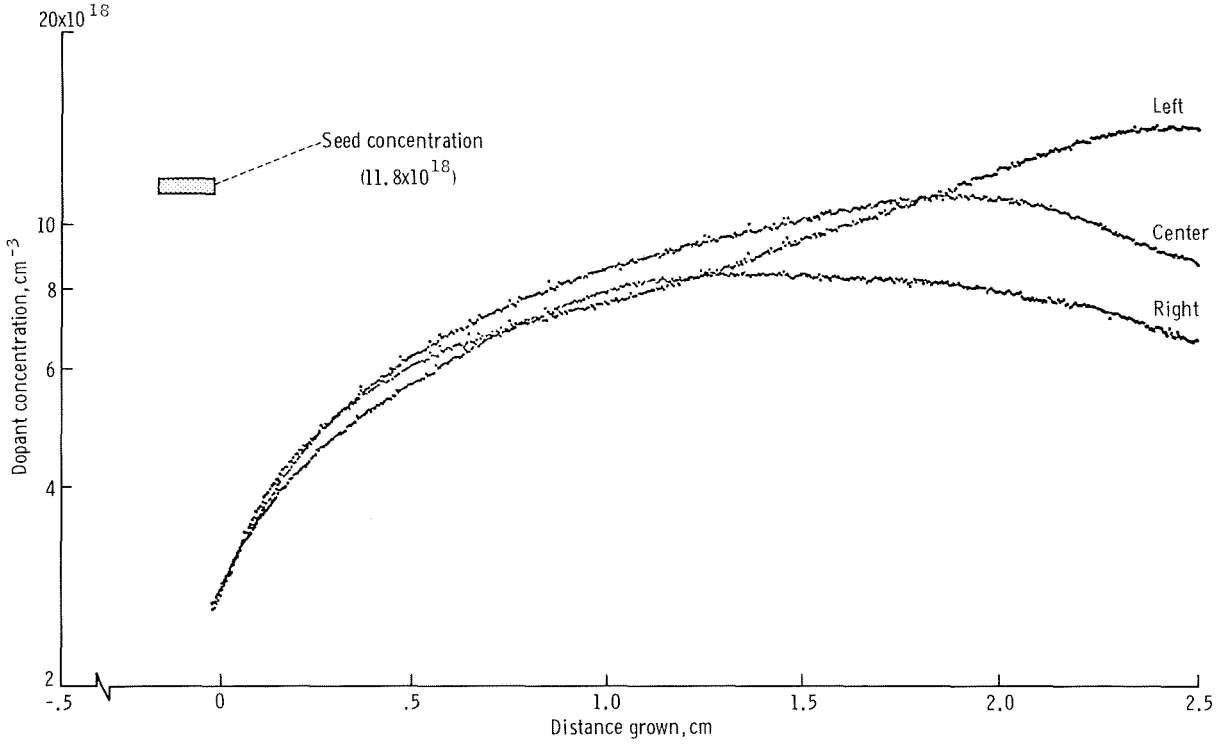

(a)

FIGURE 24-12.—Longitudinal composition profiles of Ga- and Sb-doped Ge crystals regrown in space. The three curves give the data obtained by scans performed on the left, center, and right of the investigated axial plane. (a) Ga-doped Ge crystal <111>. (b) Sb-doped Ge crystal <100>.

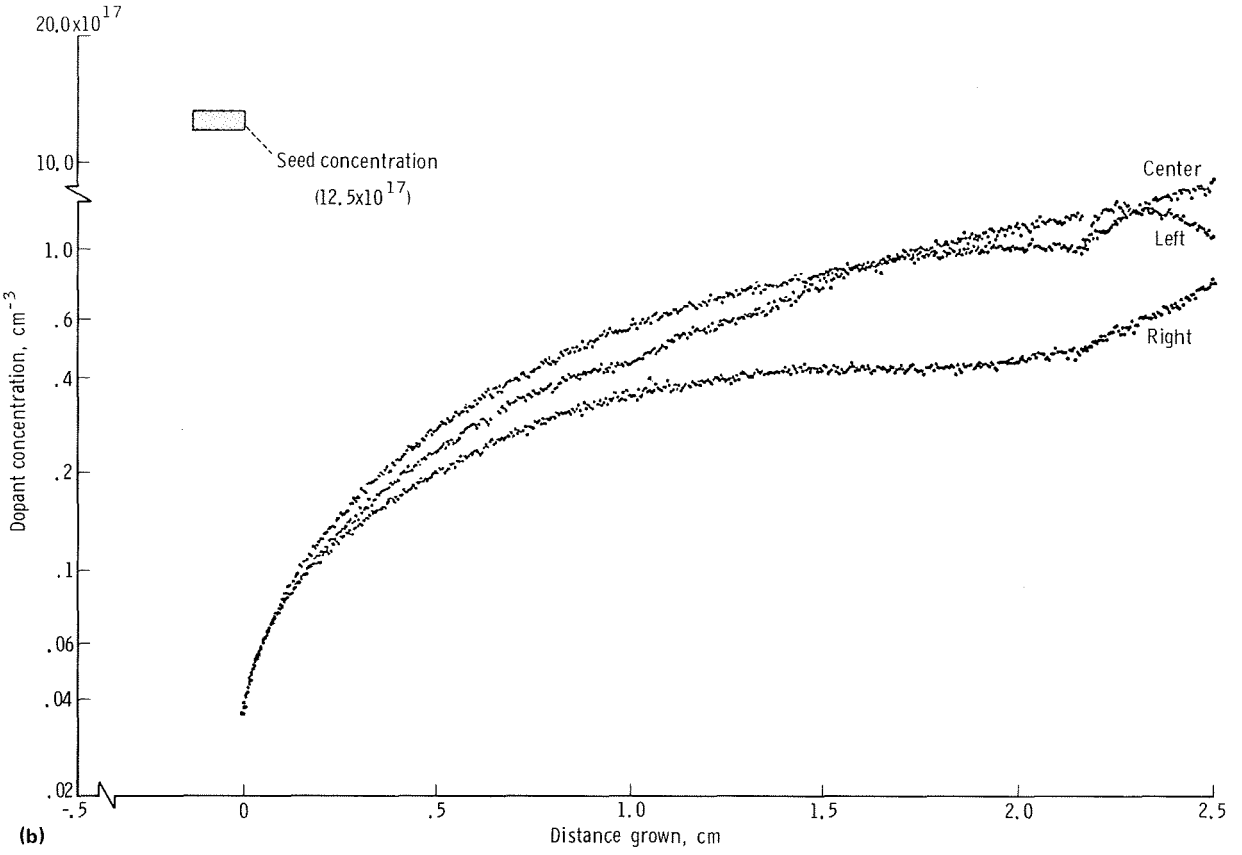

FIGURE 24-12.—Concluded.

It is self-evident that, in the presence of convective interference, the distance x from the original growth interface at which the value C_x is reached must exceed x_{max}. It is also evident that, if the critical distance x assumes any value smaller than x_{max}, the result may be interpreted as evidence for the absence of convective interference. The results of this analysis for growth of Ga-doped germanium are shown in figure 24-14.

It can be seen that the Ga concentration in the space-grown crystal reached the value C_x virtually at the calculated distance of x_{min} (0.9 cm). In contrast, in the Earth-grown crystal, the critical concentration is reached at a distance well beyond x_{max}. Thus, in spite of the uncertainty associated with the required physical constants, the present results are considered as concrete evidence of the absence of time-independent convective interference with dopant segregation. (The present analysis was not applied to the Sb-doped Ge crystals, because the critical distance is in excess of 6 cm.)

Therefore, the present analysis provides an interpretation of microsegregation and macrosegregation behavior consistent with diffusion control in the microgravity environment established during the ASTP mission. The analysis also shows that the establishment of thermal configurations leading to planar or near-planar solidification fronts is essential for the achievement of radial compositional homogeneity during crystal growth under diffusion-controlled, near-zero-g conditions.

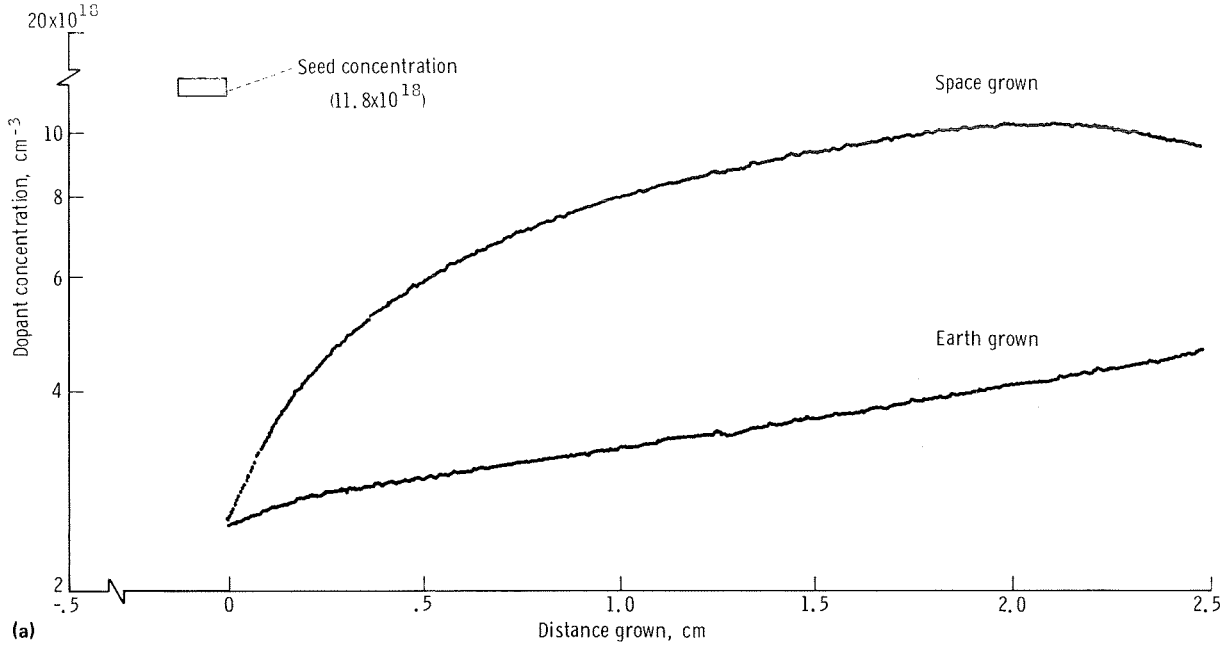

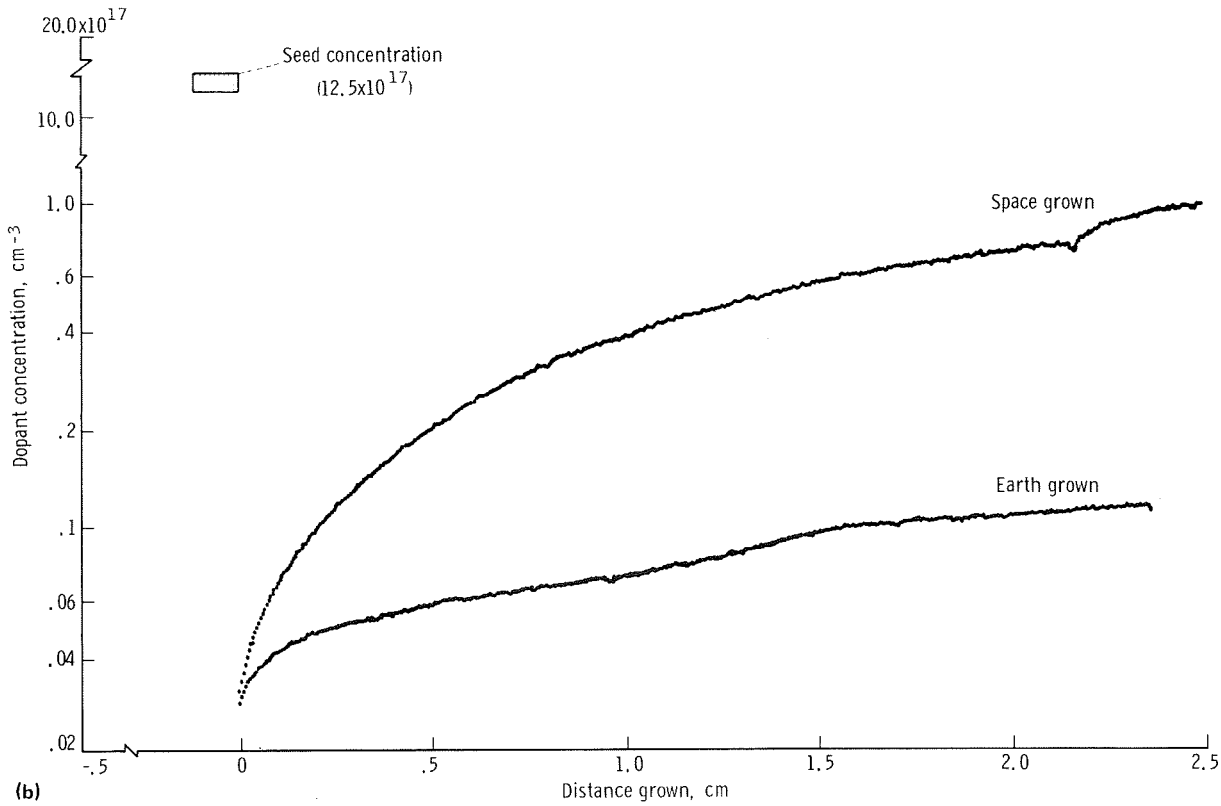

FIGURE 24-13.—Averaged longitudinal composition profiles of Ga- and Sb-doped Ge crystals regrown in space. The data constitute the average of the concentration values of the longitudinal scans shown in figure 24-12. (a) Ga-doped Ge crystal <111>. (b) Sb-doped Ge crystal <100>.

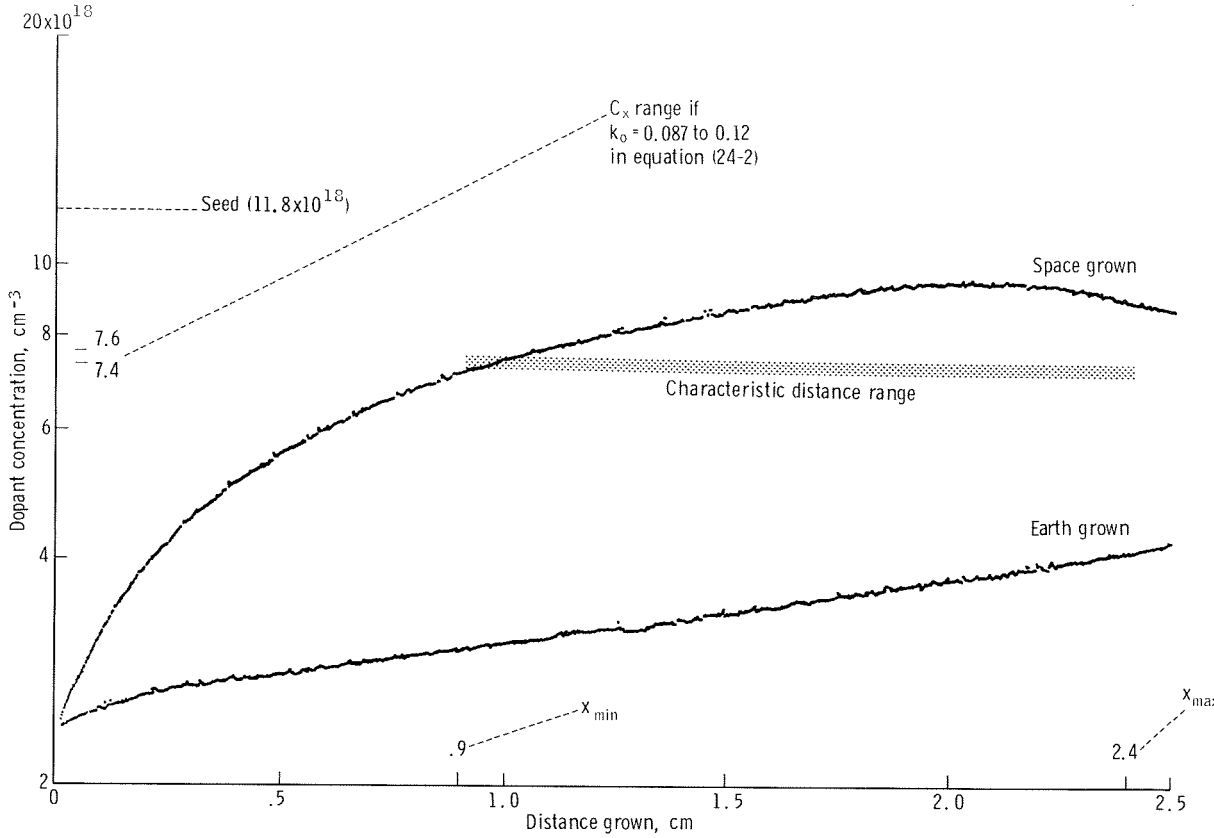

FIGURE 24-14.—Application of transient segregation theory to experimental results of figure 24-13(a). (See text.)

Appendix — Technical Information

GROWTH OF GERMANIUM CRYSTALS FOR GROUND-BASED TESTS AND FLIGHT EXPERIMENTS

The 23 germanium (Ge) single crystals that were used for the experiments were pulled from doped melts by the Czochralski technique under the following growth conditions.

1. The Ge charge was 240 g in ATJ graphite crucibles.
2. The dopant elements were gallium (Ga), tin (Sn), and antimony (Sb). (All crystals were singly doped.)
3. The melts were doped to achieve an average dopant concentration in the grown crystals of approximately 10^{18} to $10^{19}/cm^3$.
4. The seed orientation was <100> and <111>.
5. The protective gas atmosphere was hydrogen (H_2) at a pressure of approximately 101 325 N/m^2 (760 mmHg).
6. The pulling rate was 14 μm/sec for Ga-doped crystals and 7 μm/sec for Sb- and Sn-doped crystals.
7. The seed rotation was 10 rpm; the crucible rotation, 0 rpm.

The crystals (weight, ≈130 g; length, ≈15 cm; and diameter, ≈1.5 cm) were centerless ground to a diameter of 1.046 cm and cut to a length of 9.5 cm. The diameter of both ends of all crystals was reduced to 0.843 cm over a length of 2.06 cm to permit the attachment of graphite cups, which served as the current contacts for interface demarcation. The crystals were subsequently etched in CP-4 (five parts nitric acid (HNO_3), three parts hydrofluoric acid (HF), three parts acetic acid (CH_3COOH), and bromine (Br_2)) to the desired diameter of 0.838 cm. Samples from both ends of all crystals were retained for determining the doping levels.

AMPOULE DESIGN AND ASSEMBLY

The ampoules confining the growth systems were constructed of heavy-wall quartz tubing (10 mm internal diameter, 16 mm outer diameter), which was centerless ground to a diameter of 1.50 cm and cut to a length of 12.7 cm. Before assembly, the ampoules were etched with HF, rinsed with distilled water (H_2O), methanol, and acetone, and dried with hot filtered air. The graphite contact cups, machined to yield low-contact resistance with the Ge crystals, were fired at 1873 K (1600° C) in a vacuum of 13.3 $\mu N/m^2$ (10^{-7} torr). The platinum leads were then attached.

The decision was made to use an open ampoule configuration (non-vacuum tight) with 0.10-cm (0.04 in.) platinum current leads and graphite cups at both ends of the crystals as contacting media. The inside length of the graphite cups was 2.0 cm, and they were designed to ensure contact with the melt irrespective of the degree of backmelting. The mechanical contact design required precision machining of the graphite cups and the Ge crystals. The ampoule design was tested in ground-based experiments and was used for the flight experiment without modification.

PULSE POWER SUPPLY

The results from preliminary experiments showed that growth characterization on a microscale through interface demarcation would require a power supply capable of delivering current pulses of the following characteristics.

1. A pulse-repetition rate of 2 seconds
2. A pulse duration of ≥ 75 milliseconds
3. An amplitude of 25 A independent of load-resistance variations up to 1 ohm

The basic design criteria of the pulse power supply and its connection to the three growth ampoules in either parallel, series, or multiplexed (sequential) configurations were evaluated. On the basis of the power available for the MA-060 experiment, a prototype unit to be connected in series with the growth ampoules was designed that delivered 50-millisecond half-width constant current pulses of 15 A amplitude into a resistive load up to 1 ohm with a nominal 4-second repetition rate. The pulse transit time was degraded to 10 milliseconds to minimize electrical isolation requirements for the spacecraft power bus.

SAMPLE PREPARATION

For bulk crystal analysis by interference-contrast microscopy and spreading-resistance measurements, all crystals were cut along the growth direction to obtain 0.2-cm-thick slices containing the crystal axis. These center cuts were mounted on brass disks and the surfaces were ground with a 10-μm abrasive. All samples were subsequently mechanically polished to a Linde A (0.3 μm) surface finish and chemically polished with a modified Syton HT 30 solution (200 ml of Syton HT 30, 200 ml of H_2O, 5 ml of H_2O_2, and 2 ml of CH_3COOH). The samples were then etched by immersion for 5 to 8 seconds in a solution of one part HF, one part CH_3COOH and one part H_2O. For quantitative segregation analysis, the specimens were first subjected to spreading-resistance measurements and subsequently investigated by interference-contrast microscopy. This procedure enabled the determination of the microscopic growth rate (from the spacing of consecutive interface demarcation lines) corresponding precisely to the region for which the dopant concentration profile was obtained by the spreading-resistance measurements (the traces of the spreading-resistance probe are visible in interference contrast). Photomicrographs were taken using Contrast Ortho Film (125 ASA).

SPREADING-RESISTANCE MEASUREMENTS

The functional relationship between resistivity and spreading resistance, with its application to the "spreading resistance probe" technique, has been described by Mazur and Dickey (ref. 24-4). Resistivity and mobility data for Ge at 573 K (300° C) were analyzed by least-squares methods and plotted as a function of impurity concentration (ref. 24-5). This procedure results in the establishment of an exact correlation between spreading resistance and impurity concentration. Thus, spreading-resistance measurements provide a precise method for determining dopant impurity profiles on a microscale (ref. 24-2).

All measurements were obtained with a single probe, which was calibrated against a small segment of the Ge $<111>$ flight crystal (0.4 by 0.4 by 0.2 cm) as a standard. The resistivity and carrier concentration of the crystal were determined by Hall-effect measurements at 573 K (300° C) using the Van der Pauw technique (ref. 24-6).

Center slices (0.2 cm thick) were cut with a diamond-wheel from the space-grown crystals and from the corresponding ground-based test crystals. Because of the 2.5-cm traverse limit of the X-axis drive of the probe positioner, each slice had to be cut, which prevented continuous scanning of the sample surfaces.

Large-area ohmic contact to the back side of all samples to be analyzed was made with an evaporated and microalloyed silver layer. The samples were pressure bonded to brass disks using conductive silver paint. The samples were then polished and etched.

Reproducibility of the measurements obtained on stabilized surfaces was better than 2 percent for the $<111>$ Ge segments and approximately 5 percent for the $<100>$ Ge segments (worst case). Occasional excessive data scatter or systematic drift of the data base could, in all cases, be traced to steps in the sample preparation.

The raw spreading-resistance data were first converted to normalized resistances using a quadratic regression fit, correcting for additional distributed resistances in the external circuitry. Resistivities were calculated from these values without smoothing and were fitted to a computer-generated expression for the concentration-to-resistivity relationship using a spline cubic interpolating polynomial. The resulting concentration values as a function of distance were plotted on a high-speed digital plotter.

REFERENCES

24-1. Morgenthaler, George W.; and Simonson, G. E., eds.: Skylab Science Experiments. Science and Technology, vol. 38, American Astronaut. Soc., 1975.

24-2. Witt, A. F.; Lichtensteiger, M.; and Gatos, H. C.: Experimental Approach to the Quantitative Determination of Dopant Segregation During Crystal Growth on a Microscale: Ga Doped Ge. J. Electrochem. Soc., vol. 120, no. 8, Aug. 1973, pp. 1119-1123.

24-3. Tiller, W. A.; Jackson, K. A.; Rutter, J. W.; and Chalmers, B.: The Redistribution of Solute Atoms During the Solidification of Metals. Acta Met., vol. 1, 1953, pp. 428-437.

24-4. Mazur, R. G.; and Dickey, D. H.: A Spreading Resistance Technique for Resistivity Measurements on Silicon. J. Electrochem. Soc., vol. 113, no. 3, Mar. 1966, pp. 255-259.

24-5. Irvin, J. C.; and Sze, S. M.: Resistivity, Mobility and Impurity Levels in GaS, Ge, and Si at 300 Deg. K. Solid-State Electronics, vol. 11, 1968, pp. 599-602.

24-6. Van der Pauw, L. J.: A Method of Measuring Specific Resistivity and Hall Effect of Discs of Orbiting Shape. Phillips Res. Rep., vol. 13, no. 1, Feb. 1958, pp. 1-9.

BIBLIOGRAPHY

Brice, J. C.: The Growth of Crystals From Liquids. North-Holland Publishing Co. (Amsterdam), 1973.

Chalmers, Bruce: The Principles of Solidification. John Wiley & Sons, Inc., 1964.

Gilman, J. J., ed.: The Art and Science of Growing Crystals. John Wiley & Sons, Inc., 1963.

Witt, A. F.; Gatos, H. C.; et al.: Crystal Growth and Steady-State Segregation Under Zero Gravity: InSb. J. Electrochem. Soc., vol. 122, no. 2, Feb. 1975, pp. 276-283.